High-altitude Venus ionosphere

R. N. Singh* and Hari Om Upadhyay
Department of Applied Physics, Banaras Hindu University, Varanasi 221005, India
*Present address: MPI für Aeronomie, Postfach 20, D-3411 Katlenburg-Lindau, FRG

Electron density and electron temperature measured by electron temperature probe (OETP) and magentic field measured by magnetometer (OMAG) have been analysed to show occasional lifting of the Venus ionosphere. The lifting up of the Venus ionosphere has been interpreted in terms of solar wind velocity and particle flux decrease caused by certain transient features associated with solar wind generation and emission.

In situ measurements of electron density during a typical orbit of *Pioneer Venus Orbiter* (PVO) have provided distributions of electron density and electron temperature extending up to high altitudes. A theoretical electron density profile consistent with the solar zenith angle and solar activity index of such a measurement has been computed. The vertical plasma transport velocity gradient responsible for bringing the compatibility of measured and theoretically computed electron density profiles has been obtained. The simultaneously measured magnetic field distribution and solar wind dynamic pressure variation suggest that the measurements during this typical orbit are associated with some unusual solar coronal events.

As a result of continuous probing of the Venus ionosphere and magnetosphere by PVO since December 1978, Venus has become the second best studied planet. Various measurements have revealed many new features of the ionopause, ionosphere and magnetosphere of Venus. The newly created ions in the subsolar extended Venus atmosphere, created by photoionization and charge exchange interactions with solar wind protons, are picked up by the solar wind magnetic field and undergo gyrations. These ions result in mass loading of the solar wind and piling up of the magnetic field in the solar wind as it approaches the ionopause region. This process increases the solar wind dynamic pressure and affects the magnetic field distribution in the ionopause region and pushes the ionopause to further lower altitudes[1-3]. The ionopause physically separates the two distinct types of plasma, namely the hot magnetosheath above and the cold ionosphere below. The steady-state position of the ionopause in response to the solar wind dynamic pressure is associated with the gradual downward transport of the plasma. The steady-state electron density below the ionopause is invariably redistributed as a consequence of solar wind-induced plasma transport processes. Whenever the solar wind dynamic pressure is large, the ionopause is formed at lower altitudes and larger transport velocity gradients are required for steady-state plasma distributions. However, plasma transport at higher ionospheric altitudes is inhibited by other interfering processes that are not yet precisely known. In this paper we attempt to derive the plasma transport features from PVO measurements at higher altitudes in the Venus ionosphere. This is accomplished by analysing data from one of the rare-type PVO orbits, during which the ionopause was formed at an altitude of 2800 km. The plasma transport velocity gradient profile has been computed by a reiteration program which seeks compatibility between a theoretically computed electron density profile and the measured electron density profile for PVO orbit 422. The plasma transport velocity gradient is found to be much smaller at higher altitudes. Since a theoretical estimate of transport velocity is much more involved, we have not estimated its magnitude at each altitude.

The variation of data points for subsolar electron density and the electron temperature profile for 36 PVO orbits around orbit 422 are shown in Figure 1. The electron density data points bounded by the solid lines show varying features of the electron density variations with altitude. The solid lines marked L show the nature of low-altitude ionopause formation around 300 km with a maximum span of fast electron density variations. For ionopause formation at higher altitudes the electron density profile shows at comparatively smaller electron density at lower altitudes. This trend of electron density variation becomes steeper at low altitudes and is associated with ionopause formation at higher altitude as denoted by U in Figure 1. The electron temperature corresponding to these orbits shows higher temperature with a comparatively less steep rise with increasing altitudes.

The solar wind magnetic field manifestations during the sequence of orbits 418–424 are shown in Figure 2. The magnetic field data for orbit 422 distinctly show the existence of very low magnetic fields extending up to very high ionopause altitudes[4]. The gradual increase of magnetic field prior to orbit 422 and afterwards is typical of this sequence of orbits. The electron density profile for PVO orbit 422 is shown in Figure 3. It is clearly seen that the ionopause for this orbit occurs at the unprecedented altitude of 2800 km. The electron density at 150 km altitude is approximately 3×10^5 cm^{-3}, and decreases steadily with increasing altitude. The electron density profile seems to be a combination of at least two types of slopes as shown by the upper and lower dotted lines in Figure 3. The electron density for this orbit is seen to be consistently higher compared to the VIRA model electron density[5]. In the altitude range 140–200 km, the measured electron density is slightly higher than the VIRA model electron density. In the altitude range 140–400 km, the difference between measured and model electron densities is found to increase, whereas above 400 km the model electron density gets closer to the measured density with altitude, exceeding the latter above 800 km.

In order to compare the measured electron density profile up to 2800 km with the theoretically computed electron density profile, we have obtained the steady-state electron

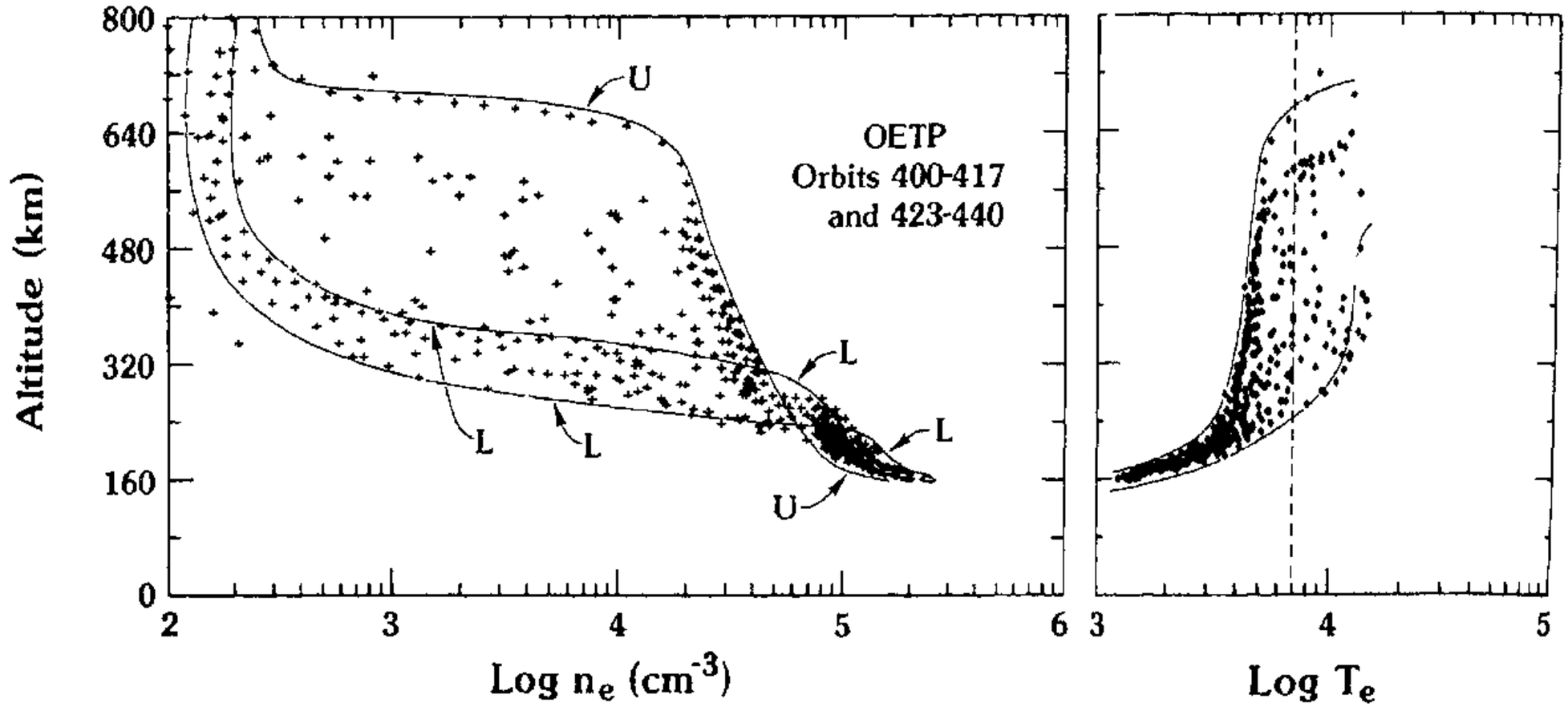

Figure 1. Electron density and electron temperature variations with altitude for 36 PVO subsolar orbits.

density profile produced by the photoionization and ion-kinetic processes. The appropriate neutral gas density profiles and ion-kinetic processes for the lower Venus atmosphere have been used[6]. Similar data for higher altitudes, though meagre, have been carefully chosen and used in this study. The electron–ion pair production rate generated by solar EUV for Venus as a function of altitude h and zenith angle χ has been computed using the well-known photoionization equation

$$q_n(h,\chi) = n_n(h) \int_0^\infty I_\infty(\lambda)\sigma_n^i(\lambda)\exp[-\tau(\chi, h)]d\lambda, \quad (1)$$

where

$$\tau(h, \chi) = \sum_n \sigma_n^a(\lambda) n_n(h) H(h) \sec \chi \quad (2)$$

and

$$H = \frac{KT}{mg} \text{ is the scale height.}$$

The appropriate Venus neutral exospheric density profiles $n_n(h)$[7,8] and I_∞, the EUV solar flux[9], have been chosen. The σ_n^a and σ_n^i in are appropriate absorption and ionization cross-sections[9–11] used in this computation. Taking various ion-kinetic equations and their appropriate reaction rates[12] with their temperature dependences, we have used the standard reiteration technique to compute the resulting electron density profile up to 3000 km (Figure 3). We find that the theoretically computed electron density profile at lower altitudes compares well with the measured OETP electron density profile as well as with the VIRA model electron density profile. The major difference between the theoretically computed electron density profile and the measured profile is seen at higher altitudes, where plasma transport, though small in magnitude, plays an important role.

We have used the steady-state continuity equation and have obtained the vertical component of plasma transport velocity gradient by seeking the compatibility of theoretically computed and measured electron density profiles at each altitude up to 2800 km. The profile dw/dz of obtained by this process is also shown in Figure 3. We find that the variation of downward and upward transport velocities is responsible for the smooth variation of the measured electron density profile of orbit 422. The downward transport velocity gradient above 1500 km is found to be much smaller. At lower altitudes the transport velocity gradient is found to be directed upwards and is comparatively more dominant. It seems that during low solar wind dynamic pressure, the lower region of the Venus ionosphere is transported upwards and the plasma at higher altitudes is transported downwards for establishment of a steady-state monotonic variation of measured electron density profile.

The sequence of PVO orbits around orbit 422 is unique in many respects. The orbits are characterized by the large occurrence of electron density and the magnetic field variations in the subsolar region. Such variations in electron density and magnetic field are not caused by mass-loading of the solar wind alone. The cause-and-effect analysis calls for an additional source producing such changes in electron density and associated magnetic field. Therefore, in addition to solar wind velocity variations, we also looked for its likely correlation with solar coronal transients. We found striking correlation with an interesting sequence of solar coronal events. During this period, the Big Bear Solar Observatory recorded three coronal holes (Table 1). The three coronal holes show fairly large southern extents. The coronal holes are characteristic of the peak of the solar maximum period and are known to be associated with high-speed solar wind[13]. In the vicinity of large coronal holes on either side of its centre, the magnetic field configuration is known to change drastically and is associated with low-speed solar wind[14]. Solar wind measurements by *Pioneer 12* showed a significant decrease in the bulk speed

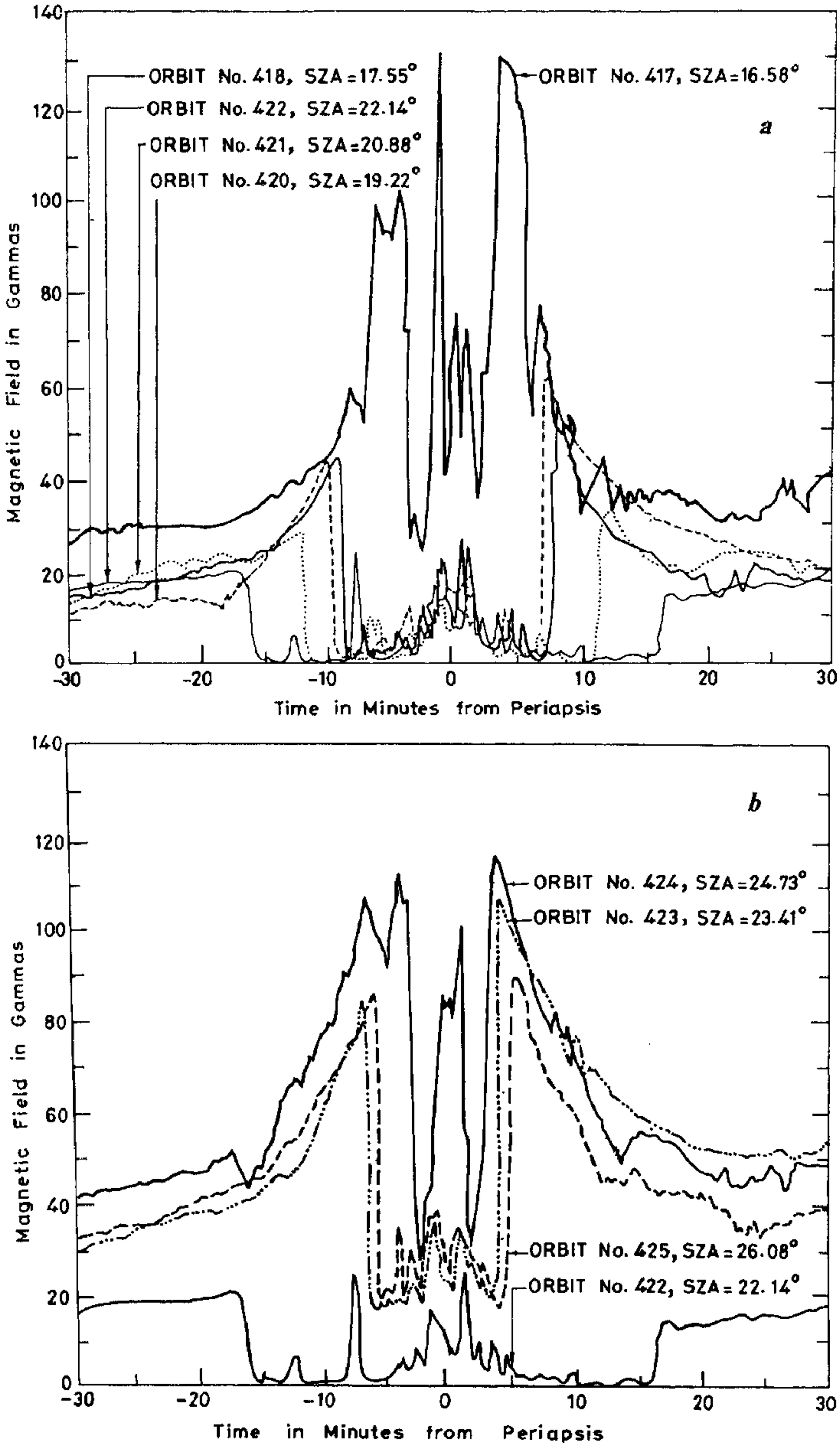

Figure 2. Total magnetic field variations during a sequence of PVO orbits including orbit 422 for which ionopause is formed at 2800 km; (*a*) orbits 417, 418, 420, 421, 422, (*b*) orbits 422, 423, 424, 425.

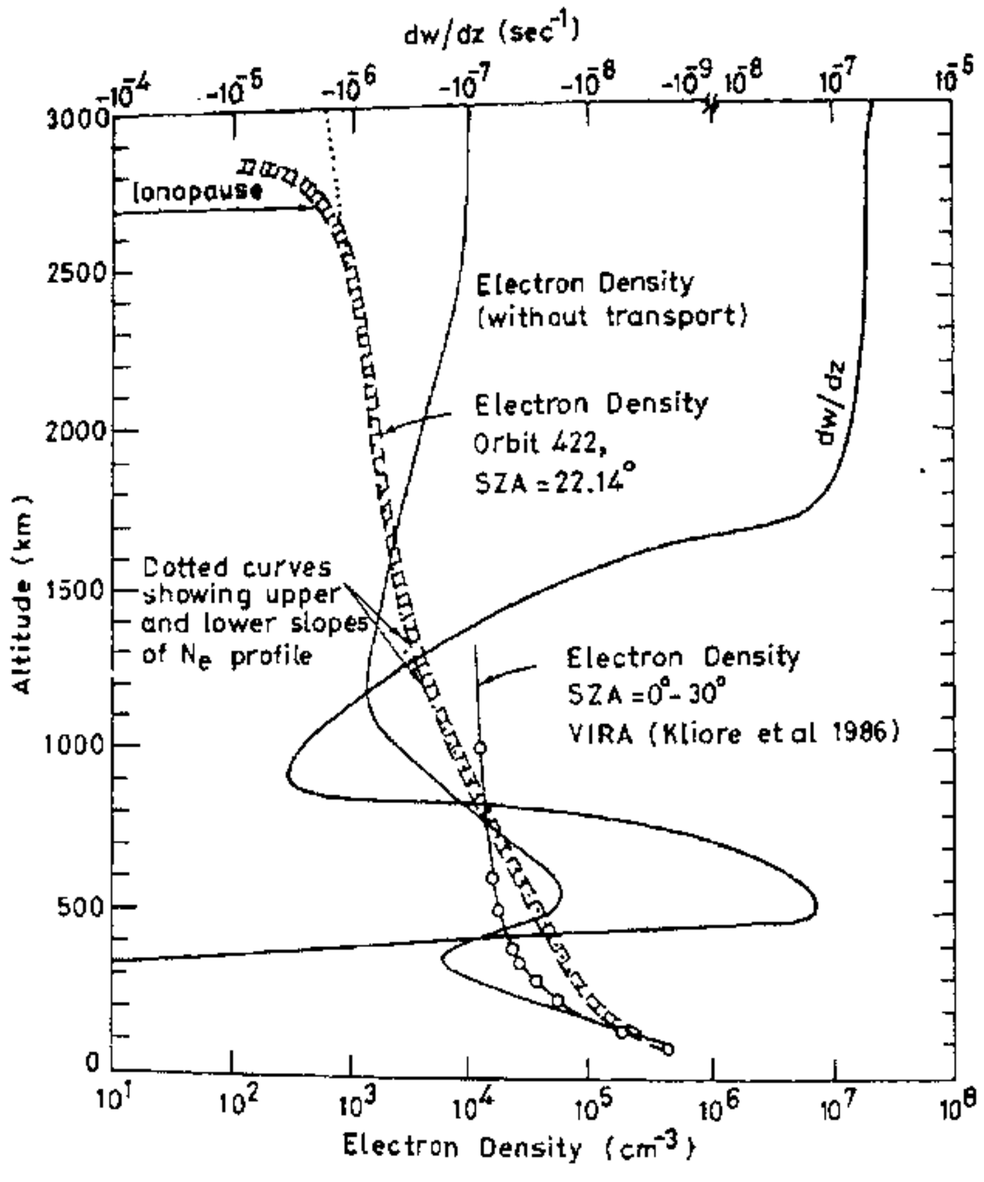

Figure 3. Computed and measured electron density profiles for PVO orbit 422 and their comparison with VIRA model electron density profile. Computed vertical velocity gradient profile for PVO orbit 422 is also shown.

Table 1. Coronal holes (GSD 1980).

Date	Extent North	Extent South	Corresponding PVO orbit
26 Jan. 1980	+48° to −5°	−140° to + 135°	417
31 Jan. 1980	+33° to +38°	−168° to +164°	422
2 Feb. 1980	+51° to +38°	−143° to 160°	424
	+21° to −43°		

and proton flux on either side of the coronal holes. Considering the reported extent of these coronal holes and spiral motion of the solar wind, we find that the relaxation time of coronal transient is in conformity with several orbit duration of PVO at 0.7 AU as revealed by magnetic field variations shown in Figure 2, *a* and *b*. The continous recording of solar wind velocity and proton flux also depict variations that may be caused by the presence of a coronal transient. We conjecture that this rare event was manifested by the coronal transient region lying in between the coronal holes which propagated and produced these unique variations in the measured electron density, magnetic field and inferred plasma transport velocity gradient during orbit 422 or PVO. This interpretation is of course speculative at present and implies that such coronal transients can originate in the region between coronal holes.

1. Ivanov-Kholodny, G. S. *et al.*, *Icarus*, 1979, **39**, 209.
2. Elphic, R. C., Russell, C. T., Slavin, J. A. and Brace, L. H., *J. Geophys. Res.*, 1980, **85**, 7679.
3. Russell, C. T. and Vaisberg, O., *Venus* (eds. Hunten, D. M., Colin, L., Donahue, T. M. and Moroz, V. I.), Tuscon, Arizona, University of Arizona Press, 1983, p. 873.
4. Luhmann, J. G., Elphic, R. C., Russell, C. T., Brace, L. H. and Hartle, R. E., *Adv. Space Res.*, 1983, **2**, 10, 17.
5. Kliore, A. J., Moroz, V. I. and Keating, G. M., *The Venus International References Atmosphere*, JPL D-2216 (1986); Also in *Adv. Space Res.*, 1985, **5**, 11, 117.
6. Schunk, R. W. and Nagy, A. F., *Rev. Geophys. Space Phys.*, 1980, **18**, 4, 813.
7. Gombosi, T. I., Horanyi, M., Nagy, A. F. and Russell, C. T., *Geophys. Res. Lett.*, 1981, **8**, 1265.
8. Chen, R. H. and Nagy, A. F., *J. Geophys. Res.*, 1978, **83**, 1133.
9. Henery, R. J. W. and McElroy, M. B., *Atmosphere of Venus and Mars*, Gordon and Breach England, 1968, pp. 251–285.
10. Hinteregger, H. E., Hall, L. A. and Schmidtke, G., *Thermosphere Space Research* V, (ed. King-Hele), North-Holland Amsterdam, 1965, pp. 1175–1190.
11. West, J. B., *Proc. R. Soc. London*, 1976, **A349**, 397.
12. Singh, R. N. and Prasad, R., *Adv. Space Res.*, 1985, **5**, 317.
13. Bohlin, J. D., *Solar Phys.*, 1977, **51**, 377.
14. Coles, W. A. and Filice, J. P., *J. Geophys. Res.*, 1985, **90**, 5082.

ACKNOWLEDGEMENT. R. N. S. thanks Prof. C. T. Russell, University of California at Los Angeles, for providing the data and for leading and beneficial discussions on the subject.

18 February 1989; revised 11 December 1989

Differential pulse polarographic study of metal ion–tetracycline binding characteristics

Sunil Sabharwal
Bhabha Atomic Research Centre, Nuclear Research Laboratory, Srinagar 190 006, India
Present address: Applied Chemistry Division, Bhabha Atomic Research Centre, Trombay, Bombay 400 085, India

The complexation tendencies of the antibiotic tetracycline with the metal ions which neutralize its antibacterial effect have been studied in acidic and neutral aqueous solutions using differential pulse polarography. The results indicate that calcium(II) and magnesium(II) ions do not bind to ring A of tetracycline while aluminium(III) and iron(III) interact with a ring A at pH 4 as well as pH 7.

It has long been known that metal ions like Ca^{2+}, Mg^{2+}, Al^{3+} and Fe^{3+} neutralize the antibacterial effect of tetracyclines on bacterial cultures[1,2]. Many techniques including spectrophotometry[3,4] NMR[5], PMR[6,7], potentiometric titrations[8] and circular dichroism[9,10] have been used to determine binding sites of tetracyclines with complexing ions but there is in general disagreement as to the specific site(s) of binding. However, it is clear that ring A plays a crucial part in complexation phenomenon.